Article

Multi-Scenario Prediction of Land-Use Changes and Ecosystem Service Values in the Lhasa River Basin Based on the FLUS-Markov Model

Bing Qi , Miao Yu and Yunyuan Li *

School of Landscape Architecture, Beijing Forestry University, Beijing 100083, China; bingqi151@bjfu.edu.cn (B.Q.); yumiao1993@bjfu.edu.cn (M.Y.)
*   Correspondence: liyunyuan@bjfu.edu.cn

Abstract: The quantitative evaluation and prediction of ecosystem service value (ESV) in the Lhasa River Basin can provide a basis for ecological environment assessment and land-use optimization and adjustment in the future. Previous studies on the ESV in the Lhasa River Basin have focused mainly on static assessment and evolution analysis based on historical data, and have not considered future development trends. Moreover, most of the current driving factors selected in land use and ESV prediction studies are homogeneous, and do not reflect the geographical and cultural characteristics of the study area well. With the Lhasa River Basin as the research focus, 20 driving factors were selected according to the characteristics of the plateau alpine area, and the land-use changes under three developmental orientations, namely, natural evolution, ecological protection, and agricultural development, were predicted for the year 2030 with the FLUS-Markov model. Based on these predictions, the values of ecosystem services were calculated, and their spatiotemporal dynamic characteristics were analyzed. The results show that the model has high accuracy in simulating land-use change in the Lhasa River Basin, with a kappa coefficient of 0.989 and an overall accuracy of 99.33%, indicating a high applicability. The types of land use in the Lhasa River basin are dominated by the existence of grassland, unused land, and forest, with a combined proportion of 94.3%. The change trends of each land-use type in the basin under the three scenarios differ significantly, with grassland, cropland, and building land showing the most significant changes. The area of cropland increased only in the agricultural development scenario; the areas of forest and grassland increased only in the ecological protection scenario; and the expansion of building land was most effectively controlled in the ecological protection scenario. The ESV increased in all three scenarios, and the spatial distribution of the ESV per unit area in the middle and lower reaches was greater than that in the upper reaches. The ESV was the greatest in the ecological protection scenario, with grasslands, forests, and water bodies contributing more to the ESV of the basin. This study provides decision-making references for the effective utilization of land resources, ecological environmental protection planning, and urban construction in the Lhasa River Basin in the future.

Keywords: ecosystem service value; land use; multi-scenario simulation; FLUS-Markov; Lhasa River basin

1. Introduction

The Lhasa River Basin, located in the middle reaches of the Yarlung Tsangpo River in the southeastern part of the Tibetan Plateau, is a key agricultural area and is the main grain production area of Tibet, China, as well as the political, economic, and cultural core of Tibet [1,2]. Notably, given that the basin is located in the core area of the ecological security barrier of the Tibetan Plateau, safeguarding the ecological security of the basin is highly important [3]. In recent years, with the intensification of climate change and human activities, the ecosystem structure and function of the Lhasa River Basin have been

affected by glacial and permafrost melting and grassland degradation, seriously impeding the sustainable development of the regional socio-economy [4–9].

Ecosystem services are any valuable functions or resources provided by ecosystems to humans that can be used directly or indirectly [10]. Ecosystem service value (ESV) is a monetary assessment of the ability of ecosystems to form and maintain the environmental conditions and material supplies on which human beings depend for survival. Currently, there are two main estimation methods for valuing ESV monetarily, namely, the method based on the price per unit of service function, and the method based on the equivalent factor of service value per unit area. Because there are many types of ecosystem services, each service function corresponds to one or more types of functional value accounting models, and each model contains a variety of parameters, the calculation burden of the functional price method, which uses the amount of ecosystem service function and the unit price to determine the total price [11], is high. Thus, the calculation process is complicated, and the difficulty of obtaining data is high. In contrast, the equivalent factor method has a harmonized value accounting model that calculates ESV by constructing the value equivalents for various service functions of various ecosystems and then combining them with the distribution area of each ecosystem [12]. Compared to the functional price method, the equivalent factor method has fewer data requirements and a simpler calculation process, and it can be quickly used to determine the total ecological value [13]. The equivalence factor method proposed by Costanza et al. [12] is one of the most commonly used methods to account for ESV [14], and is widely used because of its standardized accounting, horizontal consistency in results, and applicability to large-scale and even global-scale value assessments [15]. Xie et al. [13] improved the equivalence factor method based on Costanza's study, and constructed a table of equivalence factors for terrestrial ESV in China by synthesizing the literature research, expert knowledge, and national biomass data for China's actual situation. In recent years, ESV research on the Lhasa River Basin has focused on static assessment and evolution analysis [16–18], but there is a lack of research on ESV predictions for the Lhasa River Basin under future development trends, which limits the effectiveness of policy decision-making related to ecological protection management in the basin. Although a few scholars have carried out work on predicting the future ESV evolution for the Tibetan Plateau based on land use changes, they have not explored the details of the internal river basins due to the large spatial scales and the land-use data resolutions, which are mostly 300 m or 1 km resolutions [9,19,20]. A river basin is a large composite ecosystem composed of natural, social, and economic components, with diverse land-use types and strong ecosystem integrity [16,21]. Therefore, land use and ESV research entailing dynamic evolutionary analyses and multi-scenario predictions from the perspective of a river basin can help reveal the patterns of ESV response to land-use changes within the basin, supporting the government and other decision-making bodies in understanding the basin's future development and dynamics and enabling the formulation of effective development strategies with specific orientations of purpose.

At present, the existing land-use change prediction models mainly include the CA-Markov model [22], CLUS-S model [23,24], and FLUS-Markov model [25,26]. The first two models have good spatial extensibility and can predict the spatial distribution pattern of future land use, but the CA-Markov model lacks a cellular state transition restriction module and can simulate only a single land-use type [27], while the CLUS-S model easily ignores the possibility of the conversion of nondominant land-use types and has shortcomings regarding the land-use allocation process [26]. The FLUS-Markov model is optimized and improved based on the traditional CA-Markov model, which can simultaneously associate multiple land-use types with driving factors, incorporate complex adaptive inertia and competition mechanisms based on roulette wheel selection, and more effectively address the uncertainty and complexity caused by natural and human factors when land-use types are transformed into other types, providing higher simulation accuracy and producing results similar to the real land-use distribution [28]. The FLUS-Markov model is better than

CA-Markov and other models in terms of simulation performance [29], and is currently one of the most mainstream land-use prediction models.

Land-use change mainly manifests as changes in land-use type, pattern, and intensity that directly or indirectly affect regional ecosystem services [30,31]. Therefore, accurate simulations of land-use change are the basis for effective ESV prediction. Currently, land-use driving factors are mostly focused on elevation, slope, slope aspect, air temperature, precipitation, GDP, population density, etc. [20,32–34], and the factors used are too homogeneous and fail to reflect the natural and anthropogenic characteristics of the study area well. This research focused on the Lhasa River Basin and included 20 driving factors specific to the plateau alpine area. Utilizing the FLUS-Markov model, three scenarios—namely, the scenarios of natural evolution (NE), ecological protection (EP), and agricultural development (AD)—were established to simulate the changes in the areas of cropland, forest, grassland, waterbody, wetland, glacier snow, building land, and unused land for the year 2030. Then, the future ESV development trends in the Lhasa River basin, under a multi-scenario model, were evaluated and predicted. The objectives of this study are: (1) to quantitatively assess and predict the future land-use change and ESV of the Lhasa River Basin; (2) to establish three development scenarios to explore the future ecological and economic development paradigm of the basin; and (3) to reveal the mechanism of land-use change influence on ESV, and to inform decision-making regarding the optimization of the land-use structure and the future management of ecological protection efforts for the basin.

2. Materials and Methods

2.1. Study Area

The Lhasa River is located in the southeastern part of the Tibetan Plateau, the "third pole of the earth", and is a part of the Liang Jiang Si He in Tibet. The basin covers an area of approximately 32,471 km^2. It has an average elevation of approximately 4900 m and a plateau temperate semiarid climate. It is an important "vein" and core link in the natural ecosystem of the Tibetan Plateau, and is one of the most fragile ecological environments in Tibet. According to the topography and geomorphology of the basin and the administrative boundaries, the Lhasa River basin is divided into upper, middle, and lower reaches, with the upper reaches located in the source area of the Jiali River (including the Seni District and Jiali counties), the middle reaches in the Dangxiong Basin area (including Dangxiong County), and the lower reaches in the Lhasa River Valley area (including Linzhou County, Mozhugongkha County, Dazi District, Chengguan District, Durlong Deqing District, Quashui County, and Sangri County) [16,35] (Figure 1). The middle and upper reaches of the Lhasa River have complex topography and are mostly mountainous, and the lower reaches have open valleys, which serve as the main agricultural area and the most populated and economically prosperous area in Tibet [36,37]. In recent years, with the rapid development of economics and construction in the basin, regional development has become extremely unbalanced, the building land area has expanded rapidly, and the ecological environment of the basin has been subjected to increased interference from anthropogenic factors, which has led to tension in the human–land relations in the watershed.

2.2. Selection of Driving Factors and Data Sources

The data used in the study include those required for ESV calculation and land-use simulation. The data used for ESV calculation mainly include China's net primary productivity (NPP) data, precipitation data, and soil erosion data from 2010 to 2020. The NPP data and precipitation data were obtained from the Resource and Environment Science and Data Center of the Chinese Academy of Sciences (https://www.resdc.cn/, accessed on 25 September 2023), and the soil erosion data were obtained from the Earth Resources Data Cloud (http://gis5g.com/, accessed on 25 September 2023). The data used for the simulation of land-use change include data on land use and the drivers of land-use change. The land-use data were obtained from the Resource and Environment Science and

Data Center of the Chinese Academy of Sciences (https://www.resdc.cn/, accessed on 25 September 2023), with a spatial resolution of 30 m × 30 m. According to the research needs, each land-use type was classified into eight categories: cropland, forest, grassland, waterbody, glacier snow, wetland, building land, and unused land. We used the land-use data for 2010 as the base period data, selected the driving factors of land-use change, and used the FLUS-Markov model to simulate the land-use pattern of the Lhasa River Basin for 2020. Considering that land-use change is affected by physical and chemical conditions and multiple factors, such as natural factors, socio-economic conditions, and location [38,39], we selected three types of driving factors: physical geography, socioeconomic, and location factors. Then, we processed the driver data by using a GIS platform so as to make them consistent with the projected coordinate system and spatial resolution of the land-use data [25,40]. The driving factors for Model 1 were selected with reference to previous research experience and totaled 13, and the driving factors for Model 2 were selected based on Model 1 for the characteristics of the plateau basins and totaled 20 (Table 1 and Figure 2).
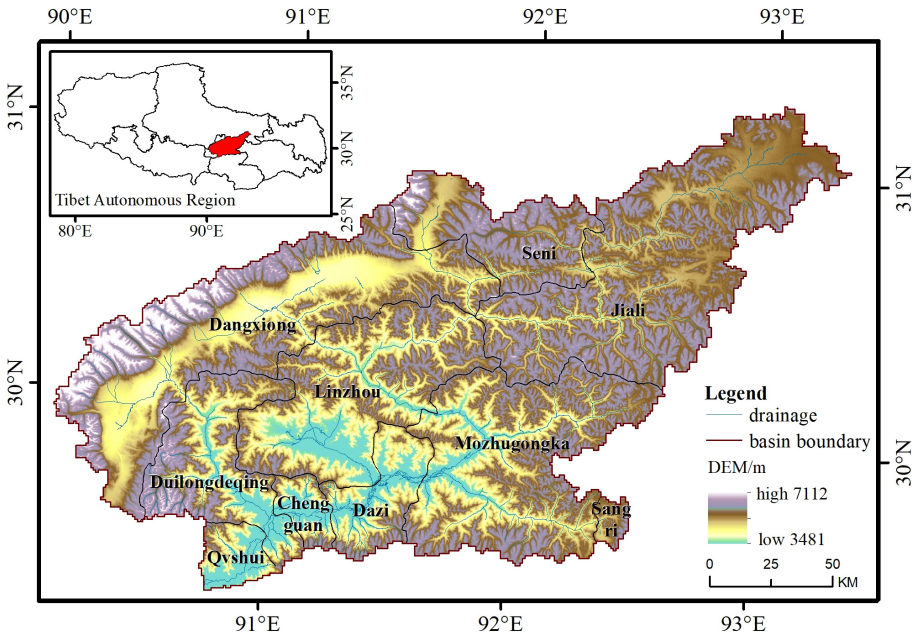

Figure 1. Location of the study area.

Table 1. Types of driving factors and data sources.

Type	Driving Factors for Model 1	Driving Factors for Model 2	Data Sources
Physical geography	DEM	DEM	Geospatial Data Cloud (https://www.gscloud.cn/, accessed on 26 September 2023)
	Slop	Slop	Extraction based on DEM data using the GIS platform
	Aspect	Aspect	
	Average precipitation	Average precipitation	Resource and Environment Science and Data Center of the Chinese Academy of Sciences (https://www.resdc.cn/, accessed on 25 September 2023)
	Average temperature	Average temperature	
		Long wave radiation	National Tibetan Plateau Scientific Data Center (https://data.tpdc.ac.cn/home, accessed on 30 September 2023)
		Shortwave radiation	
		Surface air pressure	
		Surface oxygen content	
		Relative humidity	
		Wind speed	

Table 1. *Cont.*

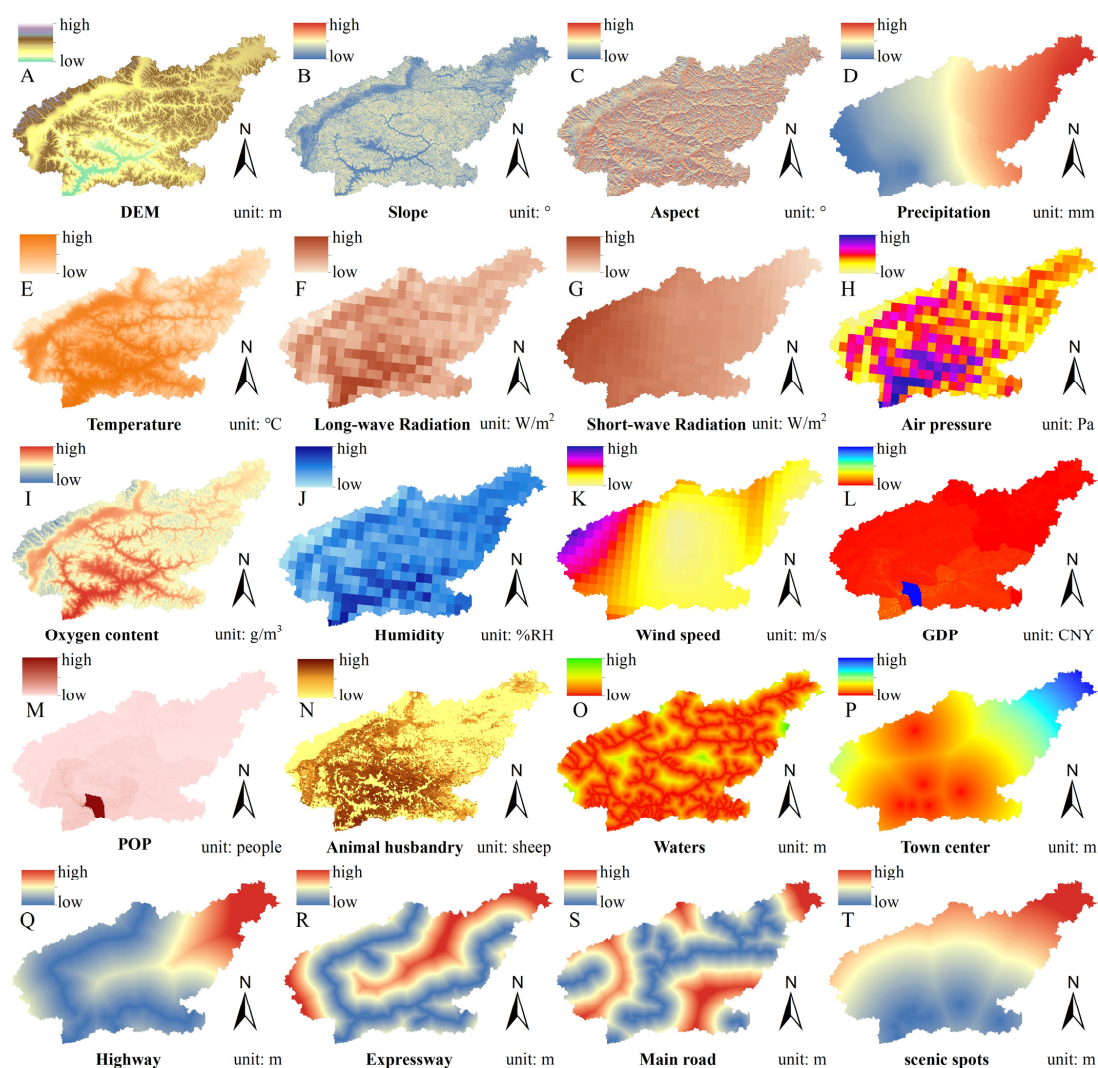| Type	Driving Factors for Model 1	Driving Factors for Model 2	Data Sources
Socio-economic	GDP	GDP	Resource and Environment Science and Data Center of the Chinese Academy of Sciences (https://www.resdc.cn/, accessed on 25 September 2023)
	Population density	Population density	WorldPop (https://www.worldpop.org, accessed on 25 September 2023)
		Livestock intensity	National Earth Observation Data Center (https://www.chinageoss.cn/, accessed on 27 September 2023)
location	Distance to waters	Distance to waters	OpenStreetMap (https://www.openstreetmap.org/, accessed on 25 September 2023) Extracted using the Euclidean distance tool in the GIS platform
	Distance to the town center	Distance to the town center	
	Distance to highway	Distance to highway	
	Distance to urban expressway	Distance to urban expressway	
	Distance to urban primary roads	Distance to urban primary roads	
	Distance to A-level scenic spots	Distance to A-level scenic spots	

Figure 2. Driving factors of land use.

In model 2, with a focus on physical geography, in addition to selecting conventional factors such as air temperature and precipitation, we also considered the special climatic type of the plateau alpine area and added factors such as surface air pressure, solar radiation, surface oxygen content, relative humidity, and wind speed, which increase the number of climate drivers and play important roles in the topography, hydrology, soil, plant growth, and distribution [41–46]. From a socio-economic perspective, considering that agriculture is the core green development industry in the Lhasa River Basin [38], we added the livestock intensity factor. The simulation results of model 1 and model 2 were compared and analyzed with the actual land-use pattern map in 2020, and the validity of the models were verified by the kappa coefficient and overall accuracy (OA). Then, the model with the higher accuracy was chosen to predict the land-use pattern in 2030 with the land-use data of 2020 as the base period data.

2.3. Simulation of Land-Use Changes
2.3.1. FLUS-Markov Model

The FLUS model is composed of a occurrence probability calculation module and a cellular automata (CA) module. In the simulation process, the artificial neural network (ANN)-based probability calculation module generates the suitability probability of each land-use type by associating the base period land-use data with various driving factors [47]. The cellular automata based on the adaptive inertial competition mechanism includes neighborhood influence factors and conversion costs, and is combined with the suitability probability of each land-use type and the total amount of future demand elements to obtain the overall probability of cellular conversion. Finally, roulette wheel selection is used to determine whether a land-use type conversion occurs in each cell [27] in order to realize the simulation and prediction of future land-use change.

Under different scenarios, the future demand of each land-use type is inconsistent, and the cellular automaton module of the FLUS model requires the input of the quantity and scale of each future land-use type in advance. Therefore, the future demand of each land-use type should be predicted in advance when applying the FLUS model. The Markov model is an effective quantitative prediction model used to predict land-use change based on a transfer probability matrix between land use states over many years. However, although it lacks consideration of land-use change in space, it can complement the FLUS model. Its calculation formula is as follows [23]:

$$S_{t+1} = P_{ij}S_t \tag{1}$$

In the formula, S_t and S_{t+1} are the land use type states at time t and time $t + 1$, respectively, and P_{ij} is the probability of land-use type conversion at time t.

- Neighborhood influence factor: The neighborhood influence factor reflects the interaction between different land-use types and the mutual influence of each land-use unit within the neighborhood [48]. In this study, the cell neighborhood window of 3 × 3 is selected, and the formula is as follows:

$$\Omega_{p,k}^t = \frac{\sum_{N \times N} con\left(c_p^{t-1} = k\right)}{N \times N - 1} \times W_k \tag{2}$$

In the formula, $\Omega_{p,k}^t$ is the neighborhood influence factor of cell p at time t; $\sum_{N \times N} con\left(c_p^{t-1} = k\right)$ is the total number of cells of land-use type k in the neighborhood in the last iteration, i.e., time $t - 1$; W_k is the neighborhood factor parameter of different land-use types. The neighborhood factor parameter indicates the expansion intensity of each land-use type [47,49], reflecting the expansion capacity of different types of land use under the influence of spatial driving factors. The parameter range is 0–1, and the closer the value is to 1, the stronger the expansion capacity of the land-use type. According to the influence of human disturbance in different regions and the historical area change trend of

each land-use type, we conducted several tests and adjustments and finally set the domain weight parameters assigned with high simulation accuracy (Table 2).

Table 2. Multi-scenario neighborhood factor parameters.

Scenario Settings	Cropland	Forest	Grassland	Waterbody	Glacier Snow	Wetland	Building Land	Unused Land
NE	0.3	0.3	0.4	0.5	0.2	0.5	0.8	0.1
EP	0.3	0.7	0.8	0.7	0.4	0.7	0.3	0.1
AD	0.8	0.3	0.3	0.4	0.2	0.5	0.6	0.1

- Setting the Conversion Cost Matrix: This study uses empirical judgment and expert consultation, combined with the development needs of three scenarios, to construct a conversion cost matrix (Table 3). When one land-use type is not allowed to be converted to another, the corresponding value is set to 0; when the conversion is allowed, it is set to 1. In addition, some land-use types with specific purposes, such as national parks, generally do not undergo land-use type conversion [50], and in this study, nature reserves and reservoirs were selected as the areas in which to restrict conversion.

Table 3. Multi-scenario conversion cost matrix.

Land Use Type	NE								EP								AD							
	a	b	c	d	e	f	g	h	a	b	c	d	e	f	g	h	a	b	c	d	e	f	g	h
a	1	1	1	1	1	1	1	1	1	1	1	1	1	1	1	1	1	0	0	0	0	0	0	0
b	1	1	1	1	1	1	1	1	0	1	0	0	0	0	0	0	1	1	1	1	1	1	1	1
c	1	1	1	1	1	1	1	1	0	0	1	0	0	0	0	0	1	1	1	1	1	1	1	1
d	1	1	1	1	1	1	1	1	0	0	0	1	1	1	0	0	1	1	1	1	1	1	1	1
e	1	1	1	1	1	1	1	1	0	0	0	1	1	1	0	0	1	1	1	1	1	1	1	1
f	1	1	1	1	1	1	1	1	0	0	0	1	1	1	0	0	1	1	1	1	1	1	1	1
g	1	1	1	1	1	1	1	1	1	1	1	1	1	1	1	1	1	1	1	1	1	1	1	1
h	1	1	1	1	1	1	1	1	1	1	1	1	1	1	1	1	1	1	1	1	1	1	1	1

In the above table, a is cropland; b is forest; c is grassland; d is waterbody; e is glacier snow; f is wetland; g is building land; and h is unused land.

2.3.2. Design of Multiple Scenario Simulations

A multi-scenario analysis can be used to explore and compare the results generated with different hypothetical development goals, and this method can help to formulate strategies suitable for the future development of a basin. Based on the previous literature, this study establishes three scenarios in combination with the current development status of the Lhasa River Basin and future socio-economic development planning [29,47,51].

- NE scenario: We assume that under this scenario, the development and change patterns of all land-use types for the year 2030 are consistent with the change trends of previous years, and there is no human intervention or restriction on land-use type conversion. This scenario is the basis for the other scenarios.
- EP scenario: The Tibetan Plateau is an important ecological security barrier in China and even in Asia [52], playing an important ecological role in biodiversity and carbon sequestration [53–55], and the Lhasa River Basin is an major ecological node. The EP scenario is oriented toward the ecological protection and high-quality development of the Lhasa River basin and toward adhering to green development and ecological prioritization, which can effectively prevent the degradation of forest and grassland areas and suppress the large-scale expansion of building land. In the model, the neighborhood factor of developed land is reduced to 0.3, and the transfer out of forest and grassland is strictly limited in the setting of the conversion cost matrix.

- AD scenario: Because the Lhasa River basin is limited by its geographical environment, natural resources, and other factors, since agriculture is the basis of its economic development [56], and at the same time, the Lhasa River Basin is one of the most important regions in the Tibet Autonomous Region for the implementation of the Comprehensive Agricultural Development Project [57,58]. The AD scenario can effectively slow the decreasing trend of cropland and ensure a level of economic development. In the model, the neighborhood factor of cropland is increased to 0.8, and the conversion of cropland to other land-use types is restricted in the conversion cost matrix.

2.4. Estimation of the ESV

Among the mainstream ESV calculation methods, the equivalence factor method based on unit area values comes with the advantages of lower data requirements, convenience in operation, and concision in calculations; moreover, it has been widely used in related studies. Considering the generality of this method, it was used in this study to calculate the ESV in the Lhasa River Basin. The magnitude of ecosystem service functions varies in different regions depending on their geographic locations, natural environments, biodiversity, etc. After reviewing the literature [59,60], 9 of the 12 ecosystem services assessed in this study (food production, raw materials production, gas regulation, climate regulation, environment purification, waste disposal, maintaining nutrient circulation, biological diversity maintenance, and aesthetic landscape provision) were positively correlated with biomass. Water resource supply and hydrology regulation were correlated with precipitation changes. Based on the above understanding, in this study, based on the Chinese terrestrial ESV equivalent factor table proposed by Xie et al., a one-step analysis was conducted to determine the modification of the unit area value equivalent parameters with NPP, precipitation, and soil retention adjustment factors [13] in order to obtain the ESV equivalent parameter table applicable to the Lhasa River Basin. The ESV calculation formula is [61]:

$$\mathrm{ESV} = \sum_{j}^{n} \left(\mathrm{VC_j} \times \mathrm{A_j} \right) \tag{3}$$

$$\mathrm{VC_j} = \sum_{i}^{m} \mathrm{VC_{ij}} \tag{4}$$

$$VC_{ij} = \begin{cases} P \times D \times ZVC_{i1j} \\ \quad\quad or \\ R \times D \times ZVC_{i2j} \\ \quad\quad or \\ S \times D \times ZVC_{i3j} \end{cases} \tag{5}$$

In the formula, ESV is the value of ecosystem services (CNY); VC_j is the value of ecosystem services of the *j*th land use type (CNY); A_j is the total area of the jth land use type (hm^2); VC_{ij} is the value of the ith ecosystem service of the jth land use type per unit area (CNY); ZVC_{ij} is the value equivalence factor of the ith land use type per unit area; D is the ecosystem services value of one standard equivalence factor (CNY/hm^2); P is the NPP regulator; R is the precipitation regulator; S is the soil conservation regulator; *i*1 denotes food production, raw materials production, gas regulation, climate regulation, environment purification, waste disposal, maintaining nutrient circulation, biological diversity maintenance, and aesthetic landscape provision services functions; *i*2 represents water resource supply and hydrology regulation service functions; and *i*3 denotes the soil conservation service.

2.4.1. NPP Modification Factor (*P*)

The NPP modification factor is calculated as follows:

$$P = B_l / B_g \tag{6}$$

In the formula, B_l is the average annual NPP (t·hm^2·a^{-1}) in the Lhasa River Basin from 2010 to 2020, and B_g is the average annual NPP (t·hm^2·a^{-1}) at the national scale, both of which were obtained by processing with the cell statistics tool in the ArcGIS 10.8 platform.

2.4.2. Precipitation Modification Factor (*R*)

The precipitation modification factor is calculated as follows:

$$R = W_l / W_g \tag{7}$$

In the formula, W_l is the average annual precipitation per unit area (mm·hm^{-2}·a^{-1}) in the Lhasa River Basin from 2010 to 2020, and W_g is the average annual precipitation per unit area (mm·hm^{-2}·a^{-1}) at the national scale, which were calculated by using the cell statistics tool in the ArcGIS10.8 platform based on the precipitation data provided by the Resource and Environment Science and Data Center of the Chinese Academy of Sciences.

2.4.3. Soil Retention Modification Factor (*S*)

The soil retention modification factor is calculated as follows:

$$S = E_l / E_g \tag{8}$$

In the formula, E_l is the annual average soil retention of Lhasa River Basin from 2010 to 2020 (t·hm^{-2}·a^{-1}), and E_g is the national average annual soil retention (t·hm^{-2}·a^{-1}); both of these values were calculated using the Sediment Delivery Ratio module in the inVEST model.

2.4.4. The Amount of Ecological Value of One Standard Equivalent Factor (*D*)

The ecological value of one standard equivalent factor can be regarded as the national average economic value of food production of 1 hm^2 of farmland under natural conditions [13]. Based on the sown area, yield, and average price of major crops in China from 2010 to 2020, this study calculated the ecological value of the standard equivalent factor. The calculation method is as follows:

$$D = S_r \cdot F_r + S_w \cdot F_w + S_c \cdot F_c \tag{9}$$

In the formula, S_r, S_w, and S_c represent the percentage (%) of the sown area of rice, wheat, and maize in the total sown area of the three crops from 2010 to 2020, respectively. F_r, F_w, and F_c represent the average net profit per unit area of rice, wheat, and corn in China from 2010 to 2020 (CNY/hm^2), respectively. The above data were calculated based on Formula (9) and the China Statistical Yearbook, the National Compendium of Cost and Benefit Information on Agricultural Products provided by the National Bureau of Statistics (https://www.stats.gov.cn/, accessed on 25 September 2023).

In this study, the ESV of the Lhasa River Basin was calculated based on the improved equivalence factor table and the ecosystem service value per unit of standard equivalence factor reported by Xie et al. in 2015 [13]. The land-use type corresponded to the closest ecosystem type, and the equivalence factor of the ESV per unit area of each land-use type was taken with reference to the proportion of the area of the secondary classification of ecosystems in Xie Gao Di's equivalence factor table, in which the ESV of the building land was considered 0 [13,62,63]. Combined with Equations (5)–(9), the modified ESV equivalent parameter table applicable to the Lhasa River Basin was obtained (Table 4, and the classification and definition of ecosystem service types are shown in Appendix A [13,63,64].

We calculated the ESV based on the actual land-use data in 2010 and 2020 and the simulated land-use data for the year 2030, and investigated its temporal and spatial change characteristics. To visualize the spatial distribution of the ESV evolution under each scenario for the years 2010 to 2030, we created a fishnet for the study area based on the GIS

platform, presented 3888 grid cells of 3 km × 3 km specifications, and calculated the ESV of each grid cell using a regional tabulation tool.

Table 4. Ecosystem service values (ESVs) per unit area of land-use type in the Lhasa River basin (10^2 CNY/hm^2).

Ecosystem Services		Land-Use Type						
Primary Type	Secondary Type	Cropland	Forest	Grass	Waterbody	Glacier Snow	Wetland	Unused Land
Provisioning service	Food production (FP)	23.38	7.72	10.05	18.70	0.00	11.92	0.47
	Raw materials production (RMP)	9.12	69.67	8.42	5.38	0.00	11.69	0.94
	Water resource supply (WRS)	−30.39	7.01	4.44	193.82	50.50	60.55	0.23
Regulating service	Gas regulation (GR)	16.83	101.00	35.07	18.00	4.21	44.42	1.40
	Climate regulation (CR)	22.68	95.16	36.47	53.54	12.63	84.17	3.04
	Environment purification (EP)	3.27	39.04	25.72	129.76	3.74	84.17	4.91
	Hydrology regulation (HR)	18.00	95.62	35.54	2384.73	166.70	566.49	1.64
	Waste disposal (WD)	32.50	40.21	30.86	287.80	0.00	1.87	6.08
Supporting service	Soil maintenance (SM)	34.37	93.99	52.37	21.74	0.00	54.01	3.97
	Maintaining nutrient circulation (MNC)	36.47	4.21	2.57	1.64	0.00	4.21	0.23
	Biological diversity maintenance (BD)	23.85	105.44	43.72	59.62	0.23	184.00	9.35
Cultural service	Aesthetic landscape provision (AL)	3.97	48.63	20.34	44.19	2.10	110.59	5.61
	Total	194.05	707.70	305.57	3218.92	240.11	1218.08	37.88

3. Results and Analysis

3.1. Verification of Model Accuracy

The values of the kappa coefficient and overall accuracy (OA) of the model are usually between 0 and 1, with larger values indicating higher model simulation accuracy. A comparison of the accuracy for the two models revealed that the kappa coefficient in Model 1 was 0.964, the OA was 97.87%, the kappa coefficient in Model 2 was 0.989, and the OA was 99.33%, with an improvement in the OA of 1.46%. In addition, comparing the simulation results of model 2 and model 1 reveals that the simulation results of model 2 are closer to the actual land-use pattern in 2020 (Figure 3), and the selection of supplementary driving factors for the characteristics of the plateau basin can improve the effectiveness of the model.
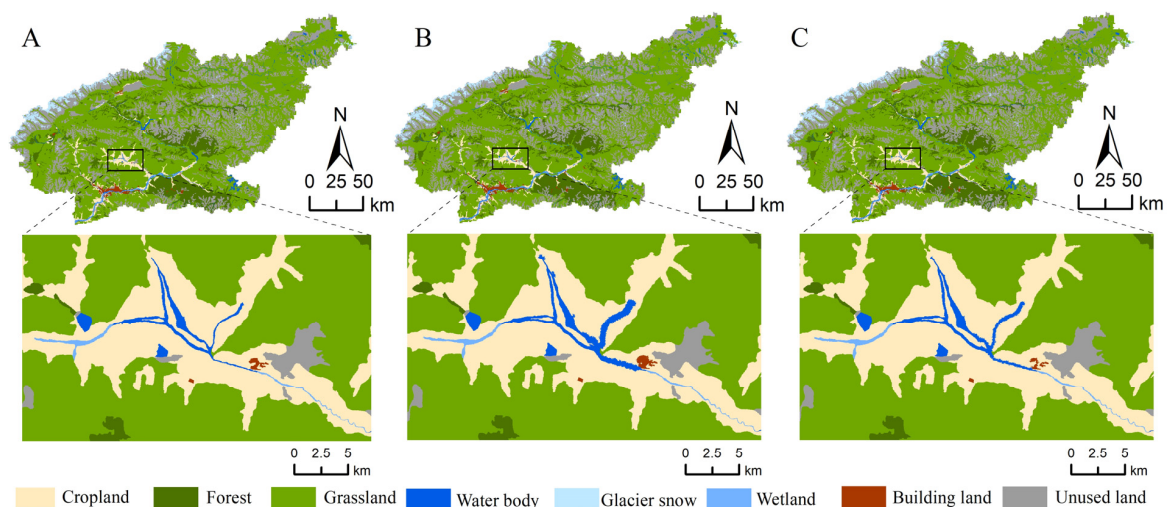

Figure 3. Actual and simulated land-use patterns in 2020. (**A**) The actual land-use pattern in 2020; (**B**) the simulated land-use pattern in 2020 of model 1; (**C**) the simulated land-use pattern in 2020 supplemented with the drivers of model 2.

3.2. Land Use Changes in the Lhasa River Basin for the Years 2010 to 2030

3.2.1. Spatial Distribution Characteristics of Land Use Types for the Years 2010 to 2030

According to the statistics for the changes in land-use types in the Lhasa River Basin for the years 2010 to 2030 (Table 5), the land-use types for the years 2010, 2020, and 2030 are mainly grassland, unused land, and forest, and the total area of the three land use types is as high as 90%. The spatial distribution patterns of different land-use types in different years are generally consistent (Figure 4). Seni District and Jiali County in the upper reaches of the Lhasa River Basin have high elevations and sparse populations, with land-use types dominated by grassland and unused land; Dangxiong County in the middle reaches is the largest pastoral county in the Lhasa River Basin [65], with grassland, unused land, and glacial snow dominating as the land-use types; the lower reaches are characterized by lower altitudes, dense populations, developing industry, agriculture, and the service economy, a rich variety of land-use types, a concentrated distribution of cropland, forest, waterbody, wetland, and building land, and a scattered distribution of grassland, glacier snow, and unused land.

Table 5. Changes in the area for different land-use types in the Lhasa River Basin for the years 2010 to 2030 (10^3 hm^2).

Time	Cropland	Forest	Grassland	Waterbody	Glacier Snow	Wetland	Building Land	Unused Land
2010	89.02	347.05	1857.51	36.85	67.50	17.57	6.02	842.96
2020	81.11	344.21	1854.26	41.07	65.43	17.60	18.36	842.47
Change rate (2010—2020) %	−8.88	−0.82	−0.17	11.43	−3.08	0.10	204.91	−0.06
2030(NE)	74.10	341.57	1851.13	44.43	64.02	17.61	29.64	841.99
Change rate (2020—NE) %	−8.64	−0.77	−0.17	8.21	−2.14	0.10	61.40	−0.06
2030(EP)	75.12	344.40	1855.22	44.55	64.70	17.60	20.94	841.99
Change rate (2020—EP) %	−7.39	0.05	0.05	8.48	−1.11	0.03	14.04	−0.06
2030(AD)	81.41	341.55	1851.08	44.00	63.70	17.61	22.99	842.18
Change rate (2020—AD) %	0.37	−0.77	−0.17	7.15	−2.64	0.11	25.18	−0.03

3.2.2. Land-Use Changes for the Years 2010 to 2020

Compared with the areas of waterbody, wetland, and building land in 2010, those in 2020 had increased by 11.43%, 0.1%, and 204.91%, respectively, and the areas of cropland, forested land, grassland, glacial snow, and unused land decreased by 8.88%, 0.82%, 0.17%, 3.08%, and 0.06%, respectively, with building land having the largest growth rate and being mainly transformed from cropland, forest, and grassland, corresponding to the largest rate of cropland area shrinkage. From a spatial point of view, the upstream area had the lowest rate of building land expansion and the lowest rate of grassland reduction, mainly because, since 2010, Tibet has accelerated the construction of the Ecological Function Protection for the Headwaters of the Lhasa River, greatly ameliorating the problem of grassland degradation in the upstream area. The changes in all land-use types (except grassland) in the downstream area were more obvious than those in the middle and upper reaches (Figure 5), which is mainly because the downstream area is the most populated and economically prosperous area, and the land-use structure is greatly influenced by human factors. The unique geographical and transportation advantages of the lower Lhasa River Basin valley, as well as the continuous expansion and adjustment of urban functions in the urban planning for the city of Lhasa, have promoted the economic development of the lower reaches and accelerated the process of urbanization. The rapid expansion of developed land has converted part of the cropland, forested land, and grassland, with the grassland being compensated for through the use of unused land and other land-use types,

such that the reduction in the grassland area has been relatively small. Overall, for the years 2010 to 2020, urban construction in the Lhasa River Basin has been effective, but the area of ecological land, such as forest and grassland, has decreased; therefore, the ecological environment is still in urgent need of protection.
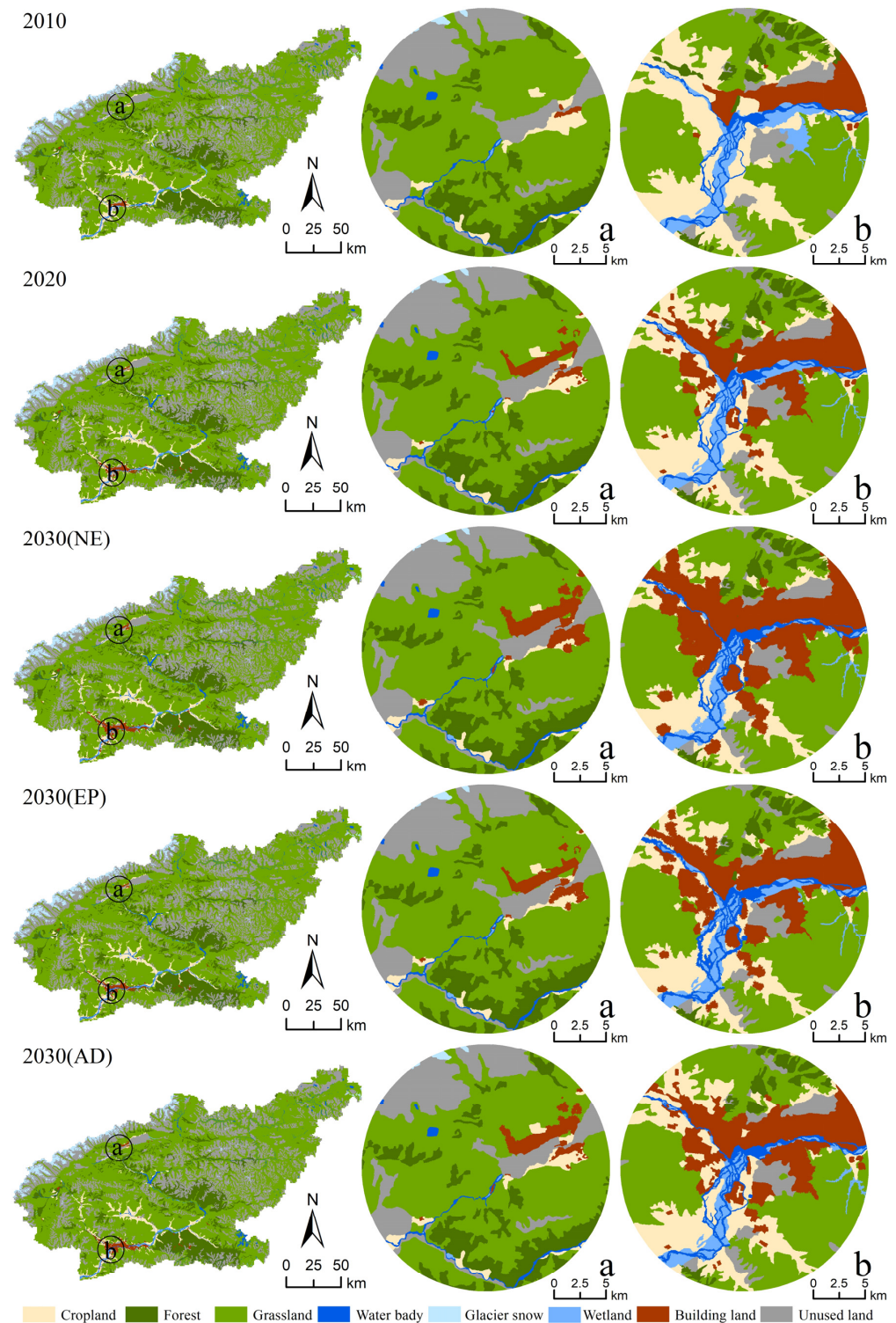

Figure 4. Land-use patterns in the Lhasa River Basin for the years 2010 to 2030: (**a**) an area located in Dangxiong county; (**b**) an area located in Dazi district.
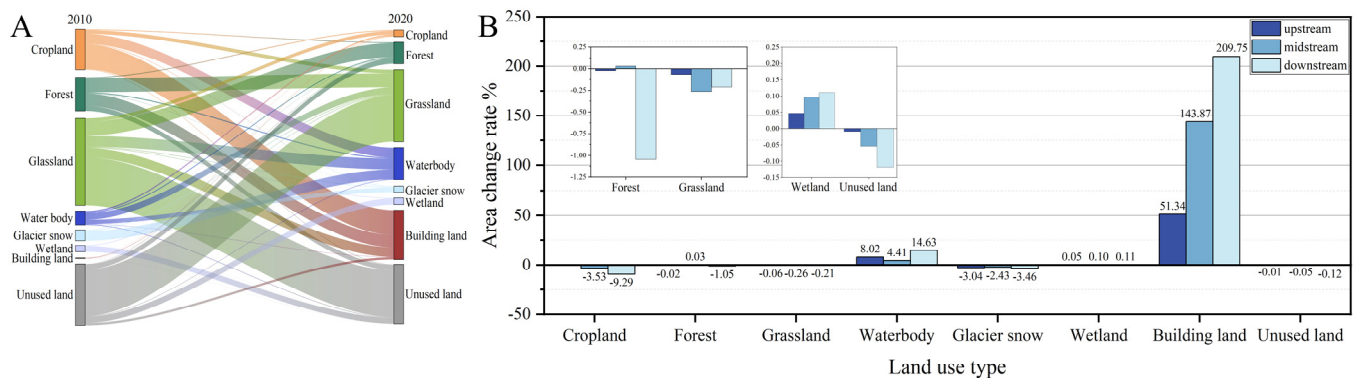
Figure 5. The (**A**) transitions between different land-use types, and (**B**) area change rates for different land-use types in the Lhasa River Basin for the years 2010 to 2020.

3.2.3. Land Use Change from 2020 to 2030

For the year 2030, in the NE scenario, the trends of area change for all land-use types continue to follow a historical pattern. In the EP scenario, there is a small increase in forest and grassland, the trend of decreasing glacial snow slows significantly, and the expansion of building land is controlled most effectively. In the AD scenario, the area of cropland grows.

- In the NE scenario, compared with the areas of waterbody, wetland, and building land in 2020, those in 2030 increased by 8.21%, 0.1%, and 61.4%, respectively, and the areas of cropland, forestland, grassland, glacial snow, and unused land decreased by 8.64%, 0.77%, 0.17%, 2.14%, and 0.06%, respectively, with the growth rate of the building land area being the largest, but slowing significantly compared with that for the years 2010–2020. The main reason for this is the limited volume the Lhasa River Basin valley area, which has fewer land resources available in a shorter period. Moreover, due to the disadvantage in geographic location compared to other developed regions in China, immigration from other cities is lower, which in turn affects the future expansion rate of building land. Spatially, the small amount of growth in grassland and a decrease in building land in the upper reaches can be attributed to the continuation of the impacts of historical policies in this scenario and the continued role of upstream ecological protection projects. The expansion of building land is still concentrated in the downstream area, continuing along the riverbank based on the original spatial distribution state (Figure 6). In conclusion, building land is still the land-use type with the largest growth rate under the influence of human activities, seriously devouring cropland, grassland, and forest. This is a trend which, if not further constrained, will greatly threaten the ecological environment and food security of the study area and impede synergistic socioeconomic–ecological development.
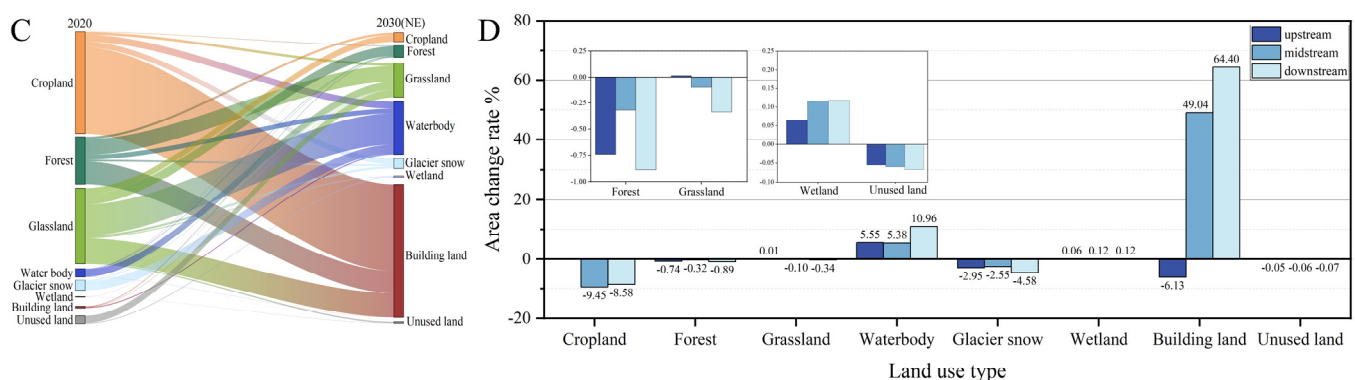

Figure 6. The (**C**) transitions between different land-use types, and (**D**) area change rate for different land-use types in the natural development scenario for the years 2010 to 2030.

- In the EP scenario, the forest, grassland, waterbody, wetland, and building land areas increased by 0.05%, 0.05%, 8.48%, 0.03%, and 14.04%, respectively, and the cropland, glacial snow, and unused land areas decreased by 7.39%, 1.11%, and 0.06%, respectively, with the expansion of building land, mainly converted from cropland, slowing markedly compared to that in the NE scenario. Due to the rapid development of economic construction in the basin, the expansion of building land is still unavoidable. However, under this scenario, its expansion rate is effectively controlled, while the land space for forest and grassland is effectively guaranteed. Spatially, the growth of forest and grassland is achieved in the upper, middle, and lower reaches, and the expansion of building land is suppressed (Figure 7). However, given the current state of land-use effectiveness in the Lhasa River Basin, the total amount of building land in the scenario may be insufficient, which will be detrimental to the economic development of the basin. Thus, the intensive and effective use of land in the basin should be strengthened in the future.
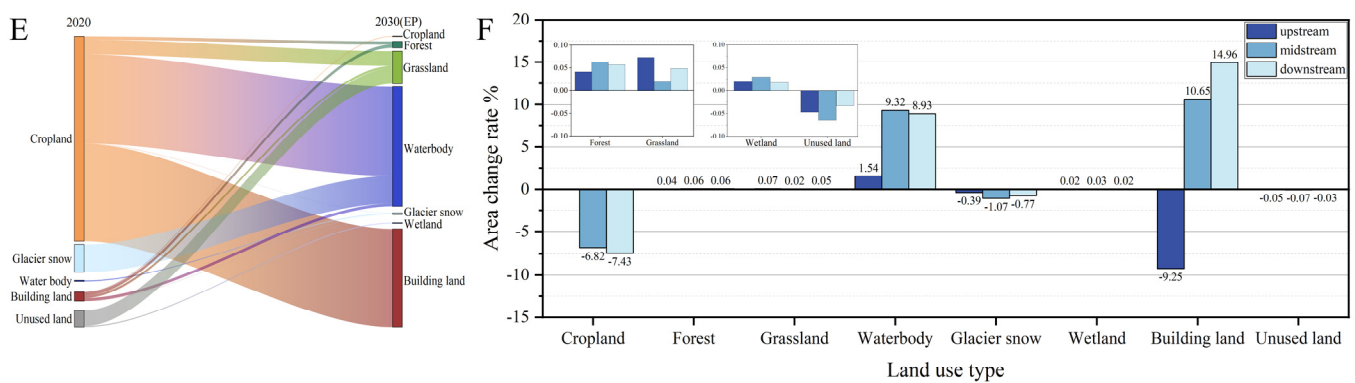

Figure 7. The (**E**) transitions between different land-use types, and (**F**) area change rate for different land-use types in the ecological protection scenario for the years 2010 to 2030.

- In the AD scenario, the areas of cropland, waterbody, wetland, and building land increased by 0.37%, 7.15%, 0.11%, and 25.18%, respectively, while the areas of forest, grassland, glacial snow, and unused land decreased by 0.77%, 0.17%, 2.64%, and 0.03%, respectively. Spatially, the cropland area in both the middle and lower reaches increased, with the most significant effect of cropland protection occurring in the lower reaches (Figure 8).
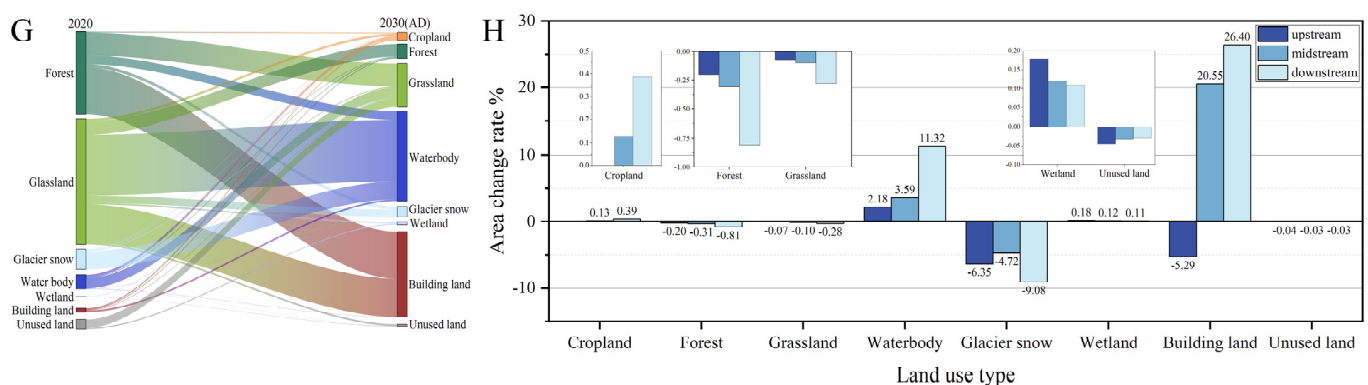

Figure 8. The (**G**) transitions between different land-use types, and (**H**) area change rate for different land-use types in the agricultural development scenario for the years 2010 to 2030.

3.3. Spatio-Temporal Variation in the ESV of the Lhasa River Basin for the Years 2010 to 2030

3.3.1. Characteristics of Temporal Variation

Based on the results of the land-use simulation, we calculated the ESV for each land-use type in 2010 and 2020 and for each scenario for the year 2030 (Table 6). The results show that the ESVs in 2010 and 2020 were CNY 102.9 billion and CNY 102.72 billion, respectively, and the ESVs in the 2030NE, EP, and AD scenarios were CNY 103.35 billion, CNY 103.75 billion, and CNY 103.34 billion, respectively, representing increases of 0.62%, 1%, and 0.61%, respectively, compared with those in 2020. The ESV shows a trend of continuous growth over time, with the largest growth rate in the EP scenario.

Table 6. Ecosystem service values (ESVs) and ESV proportions of different land-use types in the Lhasa River Basin for the years 2010 to 2030 (10^8 CNY).

Land Use Type	2010	Proportion %	2020	Proportion %	2030 (NE)	Proportion %	2030 (EP)	Proportion %	2030 (AD)	Proportion %
Cropland	17.27	1.68%	15.74	1.53%	14.38	1.39%	14.58	1.41%	15.80	1.53%
Forest	245.61	23.87%	243.60	23.72%	241.73	23.39%	243.73	23.49%	241.71	23.39%
Grass	567.61	55.16%	566.61	55.16%	565.66	54.73%	566.90	54.64%	565.64	54.73%
Waterbody	118.63	11.53%	132.19	12.87%	143.03	13.84%	143.40	13.82%	141.63	13.70%
Glacier snow	16.21	1.58%	15.71	1.53%	15.37	1.49%	15.53	1.50%	15.29	1.48%
Wetland	21.41	2.08%	21.43	2.09%	21.45	2.08%	21.43	2.07%	21.45	2.08%
Unused	31.93	3.10%	31.91	3.11%	31.89	3.09%	31.89	3.07%	31.90	3.09%
total	1029.00	100.00%	1027.18	100.00%	1033.51	100.00%	1037.47	100.00%	1033.43	100.00%

From the perspective of each land-use type, the ESVs for waterbody and wetland increased for the years 2010 to 2020, while the ESVs for all other land-use types decreased. As the first and third land-use types in terms of basin area, the ESVs for grassland and forest accounted for more than 50% and 20% of the total value, respectively, and the ranking of the ESV of each land-use type was in the order of grassland > forest > waterbody > unused land > wetland > cropland > glacial snow. For the years 2020–2030, the ESVs of the different land-use types in the NE scenario continue to follow the trends observed in the historical period. As the areas of forest and grassland in the EP scenario increase to a certain extent, the ESV increases slightly, increasing by CNY 13 million and CNY 29 million, respectively, compared with the values in 2020. In the AD scenario, the cropland ESV increases slightly, reaching CNY 5.1 million higher than that in 2020. The waterbody and wetland ESV in the 3 scenarios still increases, while the glacial snow and unused land ESV still decreases (Figure 9).
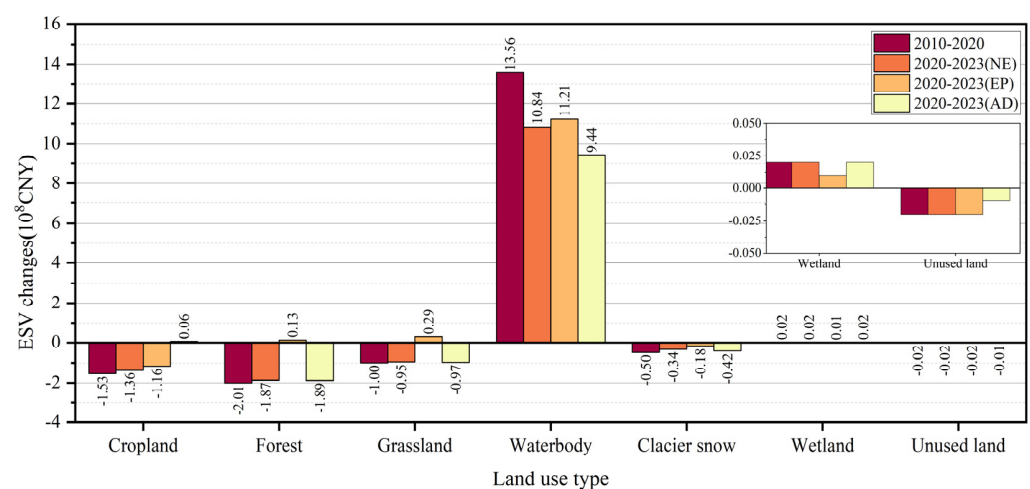

Figure 9. Changes in the ecosystem service values (ESVs) for different land-use types in the Lhasa River Basin for the years 2010 to 2030 (10^8 CNY).

In terms of individual ecosystem service types, the ESV values of each ecosystem service function in the three scenarios in 2010, 2020, and 2030 were ranked in the order of hydrology regulation > biological diversity maintenance > soil maintenance> climate regulation > gas regulation > waste disposal > environment purification > aesthetic landscape provision > raw materials production > food production > water resources supply > maintaining nutrient circulation (Table 7). From 2010 to 2020, the ESVs of water resources supply, environment purification, hydrology regulation, and waste disposal increased, while those of all other ecosystem service types decreased, with the ESV of water resources supply having the largest rate of increase and the ESV of maintaining nutrient circulation having the largest rate of decrease. From 2020 to 2030, in the NE scenario, the trend of ESV changes for individual ecosystem service types is the same as that for the years 2010–2020; in the EP scenario, there is an increase in the ESV of gas regulation, climate regulation, biological diversity maintenance, and aesthetic landscape provision; and in the AD scenario, there is a slight increase in the ESV of food production (Figure 10). The impacts of human activities on land-use structure under different scenarios are highly differentiated, and in the future, ecological protection and restoration interventions in the process of development and construction should be strengthened in the Lhasa River Basin to curb the disorderly expansion of human industry and living space.

Table 7. The ecosystem service values (ESVs) of different ecosystem service types for the years 2010 to 2030 (10^8 CNY).

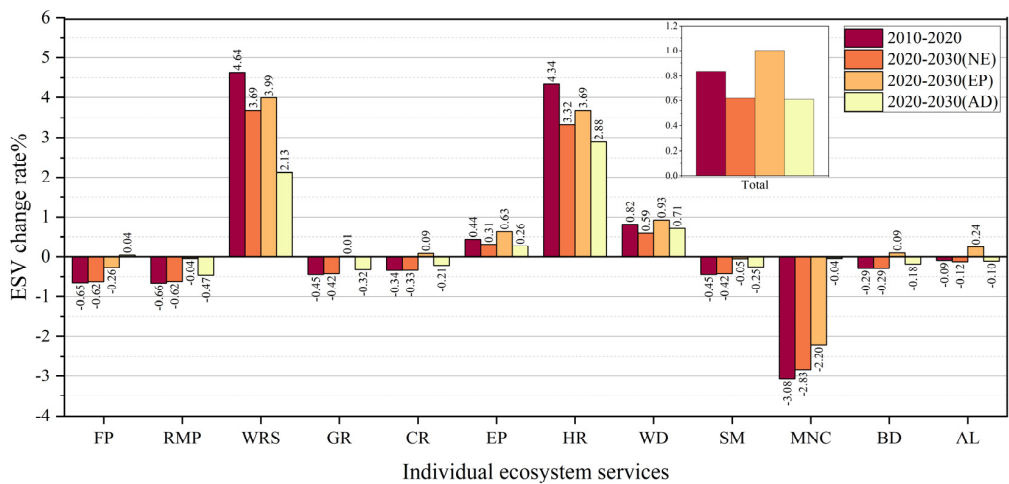| Types of Ecosystem Services	2010	2020	2030 (NE)	2030 (EP)	2030 (AD)
Food production (FP)	24.726	24.565	24.413	24.501	24.575
Raw materials production (RMP)	41.817	41.542	41.286	41.527	41.349
Water resource supply (WRS)	19.793	20.711	21.475	21.538	21.152
Gas regulation (GR)	104.604	104.136	103.697	104.147	103.807
Climate regulation (CR)	109.657	109.288	108.927	109.381	109.062
Environment purification (EP)	72.265	72.582	72.807	73.042	72.772
Hydrology regulation (HR)	211.271	220.449	227.771	228.582	226.808
Waste disposal (WD)	89.937	90.675	91.212	91.517	91.323
Soil maintenance (SM)	138.057	137.439	136.858	137.374	137.096
Maintaining nutrient circulation (MNC)	9.816	9.514	9.245	9.304	9.510
Biological diversity maintenance (BD)	133.257	132.876	132.493	132.998	132.639
Aesthetic landscape provision (AL)	63.457	63.402	63.328	63.557	63.336
Total	1018.657	1027.179	1033.512	1037.469	1033.429

Figure 10. Changes in the ecosystem service values (ESVs) of different ecosystem service types for the years 2010 to 2030.

3.3.2. Spatial Variation Characteristics

Based on the GIS platform, we used the natural discontinuity grading method to classify the ESV of the regional grid cells into five grades: lower, low, medium, high, and higher (Figure 11). Overall, the spatial distribution pattern of the ESVs in the basin for the years 2010 to 2030 basically remained unchanged, showing high spatial characteristics in the west and low spatial characteristics in the east, but with obvious changes in the ESV in some downstream areas (Figure 12). The high-ESV areas were mainly distributed in the downstream area of the basin and were concentrated in the western and southern parts of Mozhugongka County, the central and eastern parts of Dazi District, and the southern part of Dangxiong County in the middle reaches of the river. The land-use types were dominated by forest, grassland, waterbody, and wetland patches. The low-ESV areas were mainly distributed in the northern area of the middle reaches of the river basin and the upstream area, which were aligned and consistent with the spatial distribution of high-elevation areas. The land-use types were dominated by glacial snow and unused land patches. After generating the zoning statistics, the ranking of the ESV per unit area in the different areas of the basin decreased in the order of downstream > midstream > upstream for the years 2010 to 2030.
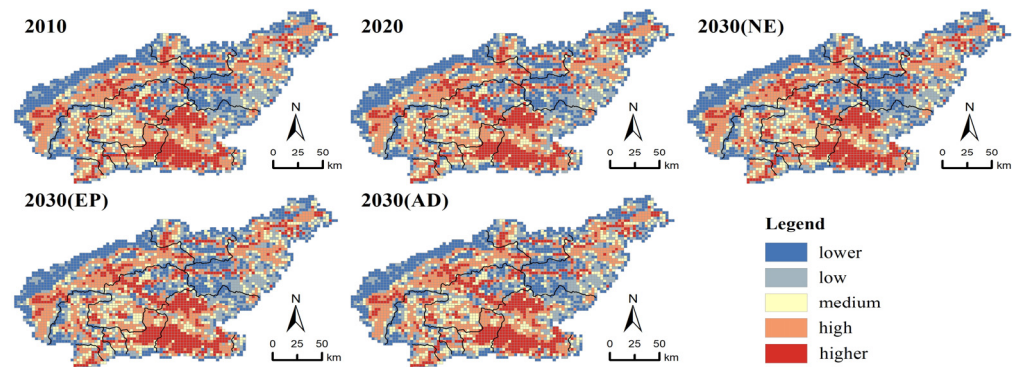

Figure 11. Spatial distribution of the ecosystem service values (ESVs) in the Lhasa River Basin for the years 2010 to 2030.
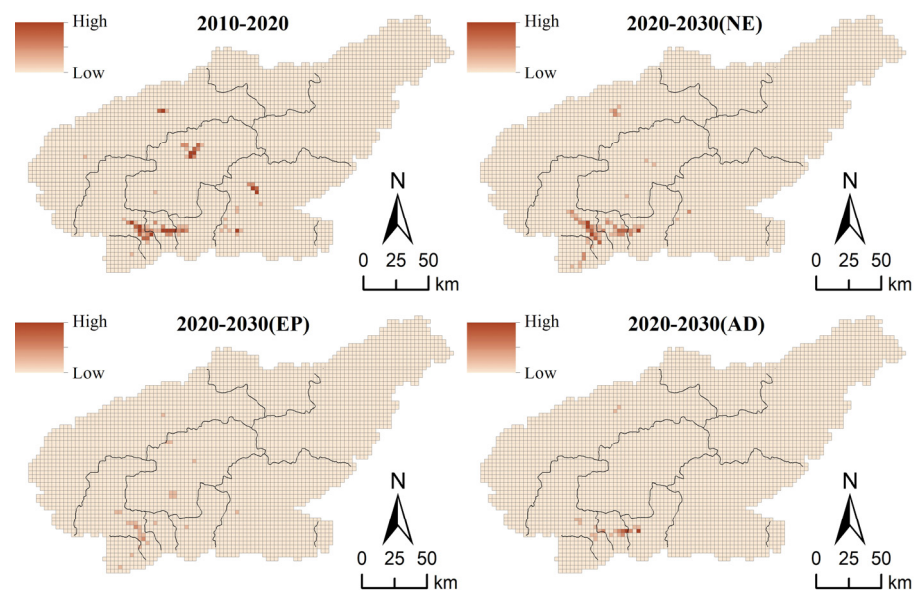

Figure 12. Spatial distribution of the degree of change in the ecosystem service values (ESVs) in the Lhasa River Basin for the years 2010 to 2030.

Statistics on the changes in ESV in different regions of the basin for the years 2010 to 2030 are shown in Figure 13. From 2010 to 2020, the ESV in the upper, middle, and lower

reaches of the basin increased; for the years 2020–2030, the ESV in the upper, middle, and lower reaches of the basin increased under both the NE and EP scenarios; and in the AD scenario, the ESV in the upper and lower reaches increased, while in the middle reaches, the ESV decreased.
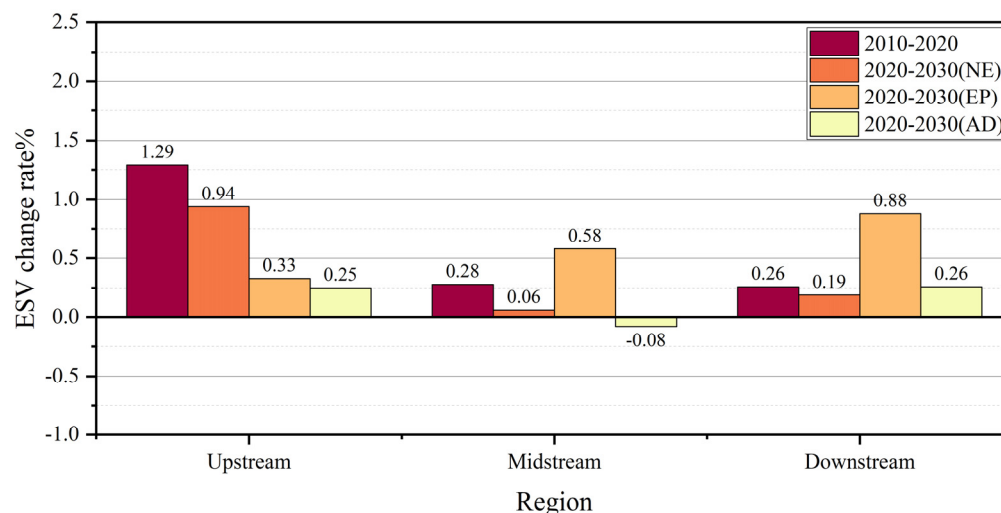

Figure 13. Changes in the ecosystem service values (ESVs) in different regions of the Lhasa River Basin for the years 2010 to 2030.

4. Discussion

4.1. Selection of Driving Factors

Land use structural change is a complex dynamic process in which multiple factors play a joint role, and it is also an important influencing factor for ESV calculations [66]. Drivers of land-use change are key factors that affect land-use modes and promote changes in land-use patterns. In this study, on the basis of the special natural environment and anthropogenic activities in the Lhasa River Basin, the driving factors were selected in a targeted way, and more climate-driving factors and livestock intensity factors were added. Through comparative analysis, we found that compared with the model without supplemented driving factors, the kappa coefficient of the model with supplemented driving factors increased by 2.5%, and the overall accuracy increased by 1.46%. This demonstrates that the targeted driving factors adapted to the characteristics of the study area play an important role in improving the prediction accuracy of the model. The selection of drivers of land-use change in this study can provide a reference for the prediction of land use change in plateau alpine basins in general.

4.2. Environmental Issues behind Land Use Type Conversion Mechanisms

The Tibetan Plateau is an ecologically fragile region of global importance, and its ecosystems are extremely sensitive to the impacts of climate change and human activities [3,67,68]. In the climatic context of global warming, its temperature has risen more than the global average has [69], which has led to accelerated glacier and permafrost melting in the Lhasa River Basin [70–72]. Glacier snowpack and unused land area exhibited a decrease for the years 2010–2030, with these areas mainly being converted to water bodies and wetlands and, in the case of some unused land, into grasslands. In the short term, permafrost melts, and surface moisture gradually increases to form wetlands, which also accelerates soil nitrogen and phosphorus mineralization and stimulates vegetation growth in permafrost areas [73–76]. The continuous increase in water resources and wetland resources in the basin seems to be a favorable response of the ecosystem. However, in the long run, the retreat of permafrost releases a large amount of greenhouse gases, accelerating global warming; moreover, when the degradation of glacier snow and permafrost reaches the

threshold, as the temperature continues to rise, the evaporation of the basin will gradually increase, and waterbody and wetland areas will face the risk of degradation [75].

4.3. Optimization Strategy Based on Land-Use Change and ESV Assessment

Based on the prediction results, under the three scenarios, cropland, forest, and grassland will continuously transition to building land instead of into each other, and if there is no human intervention in the expansion of building land, by 2030, its area will increase significantly, with an increase of 61%. Moreover, cropland, forest, and grassland will further diminish, and the food and ecological security of the basin will face a great threat. In the EP scenario, the increase in building land decreases significantly, the area of forest and grassland increase, and the ESV value is the highest among the three scenarios, making this scenario the most suitable for the development path of environmental resource protection and ecological civilization development. Although the ESV under the AD scenario is the lowest among the ESVs of the three scenarios, it still increases relative to that in 2020, indicating that this scenario can effectively promote the coordinated development of ecological protection and socio-economic development of the basin. This outcome would be consistent with the development notion of "developing an ecological economy, taking a development path that harmonizes the economy with resources and the environment, and more sustainable development" in the "14th Five-Year Plan" and "Vision 2035" for Tibet's national economic and social development.

Although the ESV of the basin as a whole is increasing, regional development is extremely unbalanced because of the large differences in land use types in different regions of the Lhasa River Basin. In the NE scenario, the growth rates of the ESV in the upper, middle, and lower reaches are lower than those of the preceding 10 years, indicating that the efficiency of the ecosystem service function of the whole basin will continue to decrease if it is allowed to develop without appropriate anthropogenic interventions. The growth rate of the ESV in the upper reaches in the EP scenario is lower than that in the preceding 10 years and that in the NE scenario, which indicates that construction of the Ecological Function Protection for the Headwaters of the Lhasa River in Tibet has had a significant effect. In the AD scenario, the ESV in the middle reaches decreases, and the analysis of its land-use type conversion reveals that the reason for this is the large reduction in grassland area.

The above analysis revealed that the changes in land use and ESV can provide a reference for the assessment of the ecological status of a basin to a certain extent. In the future protection and management of basin ecosystems, the following differentiated optimization measures should be formulated for different scenarios and regions: (1) In the EP scenario, the protection and management of upstream meadows and grasslands should be strengthened, research should be carried out on the mechanism and causes of degradation in seriously degraded areas, and targeted measures should be taken to strengthen the protection and restoration work in these areas. Additionally, high-standard and large-area afforestation projects should be carried out, and scientific and technological support should be provided for the optimization of plateau eco-afforestation and the structure of tree species, so as to form a forestry ecosystem with various levels, reasonable structure, and complete functions. (2) In the NE scenario and AD scenario, the remote sensing and positional monitoring of basin ecosystems should be increased, especially regarding the detection of dynamic changes in glacier snow in Dangxiong County in the middle reaches, and relevant research should be carried out. Furthermore, the grassland fixed monitoring point project, artificial forage land project, and degraded grassland replanting project should be implemented in the middle reaches, which has a high degree of animal husbandry. Grazing should be banned during the growing period of plants and strictly restricted during the fruiting period, so as to effectively protect and restore natural grasslands and alleviate the pressure of overloading and overgrazing in pastoralist counties. (3) As the downstream region is the area of the basin that is most affected by human interference, the dynamics of land use, ecology, and urban development in

the downstream region should be constantly monitored. The protection of downstream cropland should be strengthened to safeguard regional food security, and the relationships among socio-economic development activities, such as grazing, tourism, and resource development should be coordinated with the needs of the ecological environment. Finally, the disturbance of the plateau ecosystem by human activities should be minimized.

4.4. Limitations

Although this study well predicts the future land-use structure and ESV in the Lhasa River Basin and enriches the research on the impact of future land-use changes on ESV, there are still several shortcomings: (1) The use of Markov chains to predict the number of pixels representing future land use demand was based solely on existing land-use data; however, it lacked consideration of the impact of future policy factors. (2) Because of the complexity of the social and natural composition of building land, recent studies have not taken the ESV of building land into account. In this study, the ESV of building land was treated as 0, on the basis of previous studies; however, this affects the total ESV of the basin to a certain extent, and further research is needed to estimate the ESV of building land. (3) The three scenarios of natural evolution, ecological protection, and agricultural development cannot cover all possible future development directions of the basin, but future research can provide more powerful support for land-use simulation and ESV assessment by introducing more advanced models and setting more comprehensive simulation scenarios.

4.5. Conclusions

This study is based on the coupled FLUS-Markov model featuring the continuous adjustment and optimization of the model parameters to achieve a multi-scenario land-use simulation, and the prediction of ESV value and its spatial distribution pattern in 2030. The model kappa coefficient reaches 0.989, the simulation feasibility is high, and it can provide a reference for the future land use changes in the Lhasa River Basin.

The land-use type of the Lhasa River Basin is dominated by grassland and unused land, and the land-use changes in the basin under the three scenarios have obvious differences, among which the changes in grassland, cropland, and building land are the most significant. The area of forest and grassland under the EP scenario shows the only increasing trend, but the increase is only 0.05%. The building land in the NE scenario has the most significant expansion, which is 61.4% higher than that in 2020. The area of cropland under the AD scenario shows an effective increase compared with that under the other scenarios, with an increase of 0.23%. The area of water bodies and wetlands shows a continuous increasing trend, which corresponds to the decreases in glacier snow and unused land. In all three scenarios, the ESV of the basin shows an increasing trend, with the largest increase in the EP scenario, which is mainly due to the increase in the area of forest and grassland. The AD scenario has the lowest ESV value, but the ESV value still increases in comparison with that in 2020 because this scenario (compared to the EP scenario) effectively restrains the expansion of the building land and does not unduly restrict the urbanization process. Therefore, from the perspective of the ecological and economic development of the basin, the AD scenario may be the most suitable for the future development of the basin. However, since the natural and social development of the upper, middle, and lower reaches of the basin varies greatly, and the focus of ecological protection and economic construction and development is different, measures should be taken in a case-by-case manner and adapted to the local conditions. This study takes three scenarios emphasizing natural evolution, ecological protection, and agricultural development as the research perspectives, and provides references for the future land-use restructuring and ecosystem-service optimization in the Lhasa River Basin.

Author Contributions: B.Q.: conceptualization, methodology, data curation, writing—original draft, validation, software. M.Y.: writing—review and editing, supervision. Y.L.: writing—review and editing, funding acquisition, supervision. All authors have read and agreed to the published version of the manuscript.

Data Availability Statement: The original contributions presented in the study are included in the article, further inquiries can be directed to the corresponding author.

Conflicts of Interest: The authors declare no conflicts of interest.

Appendix A. Classification and Definition of Ecosystem Services

Ecosystem Services		Definition
Primary Type	Secondary Type	
Provisioning service	Food production (FP)	Conversion of solar energy into edible plant and animal products.
	Raw materials production (RMP)	Conversion of solar energy into bioenergy for humans to use in buildings or other uses.
	Water resource supply (WRS)	Water resources provided by various ecosystems and used for residential life, agriculture (irrigation), industrial processes, etc.
Regulating service	Gas regulation (GR)	The ecosystem maintains a balance of atmospheric chemical components, absorbing SO_2, absorbing fluoride, and absorbing nitrogen oxides.
	Climate regulation (CR)	The regulating effect on regional climate, such as increasing precipitation and lowering temperature.
	Environment purification (EP)	Vegetation and organisms retain dust, decontaminate, etc., including purifying water and air.
	Hydrology regulation (HR)	Ecosystems intercept, absorb and store precipitation, regulate runoff, regulate and store flood water, and reduce drought and flood disasters.
	Waste disposal (WD)	The role of vegetation and organisms in the removal and decomposition of excess nutrients and compounds.
Supporting service	Soil maintenance (SM)	The role of organic matter accumulation and vegetation root matter and organisms in soil conservation, nutrient cycling and accumulation.
	Maintaining nutrient circulation (MNC)	Storage, internal circulation, processing and acquisition of N, P, and other elements and nutrients.
	Biological diversity maintenance (BD)	Wildlife gene origin and evolution, wild plant, and animal habitats.
Cultural service	Aesthetic landscape provision (AL)	Landscapes with (potential) recreational use, cultural, and artistic value.

References

1. Han, W.; Su, X.; Lu, H.; Li, T.; Jin, T.; Zhang, M.; Liu, G. Impacts of human activity intensity on ecosystem services for conservation in the Lhasa River Basin. *Ecosyst. Health Sustain.* **2023**, *9*, 88. [CrossRef]
2. Wu, X.; Li, Z.; Gao, P.; Huang, C.; Hu, T. Response of the downstream braided channel to Zhikong Reservoir on Lhasa River. *Water* **2018**, *10*, 1144. [CrossRef]
3. Liu, J.; Milne, R.I.; Cadotte, M.W.; Wu, Z.Y.; Provan, J.; Zhu, G.F.; Gao, L.M.; Li, D.Z. Protect Third Pole's fragile ecosystem. *Science* **2018**, *362*, 1368. [CrossRef] [PubMed]
4. Gao, Q.Z.; Wan, Y.F.; Xu, H.M.; Li, Y.; Jiangcun, W.Z.; Borjigidai, A. Alpine grassland degradation index and its response to recent climate variability in Northern Tibet, China. *Quatern. Int.* **2010**, *226*, 143–150. [CrossRef]
5. Nie, Y.; Zhang, X.; Yang, Y.; Liu, Z.; He, C.; Chen, X.; Lu, T. Assessing the impacts of historical and future land-use/cover change on habitat quality in the urbanizing Lhasa River Basin on the Tibetan Plateau. *Ecol. Indic.* **2023**, *148*, 110147. [CrossRef]
6. Ran, Y.; Li, X.; Cheng, G. Climate warming over the past half century has led to thermal degradation of permafrost on the Qinghai–Tibet Plateau. *Cryosphere* **2018**, *12*, 595–608. [CrossRef]
7. Sun, L.; Li, H.; Wang, J.; Chen, Y.; Xiong, N.; Wang, Z.; Wang, J.; Xu, J. Impacts of climate change and human activities on NDVI in the Qinghai-Tibet Plateau. *Remote Sens.* **2023**, *15*, 587. [CrossRef]

8. Yao, T.; Thompson, L.; Yang, W.; Yu, W.; Gao, Y.; Guo, X.; Yang, X.; Duan, K.; Zhao, H.; Xu, B.; et al. Different glacier status with atmospheric circulations in Tibetan Plateau and surroundings. *Nat. Clim. Chang.* **2012**, *2*, 663–667. [CrossRef]

9. Zhou, Y.; Zhang, X.; Yu, H.; Liu, Q.; Xu, L. Land use-driven changes in ecosystem service values and simulation of future scenarios: A casestudy of the Qinghai–Tibet Plateau. *Sustainability* **2021**, *13*, 4079. [CrossRef]

10. Daily, G.C.; Postel, S.; Bawa, K.; Kaufman, L. *Nature's Services: Societal Dependence on Natural Ecosystems*; Island Press: Washington, DC, USA, 1997; p. 392. [CrossRef]

11. Campbell, E.T. Revealed social preference for ecosystem services using the eco-price. *Ecosyst. Serv.* **2018**, *30*, 267–275. [CrossRef]

12. Costanza, R.; D'arge, R.; De Groot, R.; Farber, S.; Grasso, M.; Hannon, B.; Limburg, K.; Naeem, S.; O'neill, R.V.; Paruelo, J.; et al. The value of the world's ecosystem services and natural capital. *Nature* **1997**, *387*, 253–260. [CrossRef]

13. Xie, G.D.; Zhang, C.X.; Zhang, L.M.; Chen, W.H.; Li, S.M. Improvement of the evaluation method for ecosystem service value based on per unit area. *J. Nat. Resour.* **2015**, *30*, 1243–1254.

14. Shi, Y.; Feng, C.-C.; Yu, Q.; Guo, L. Integrating supply and demand factors for estimating ecosystem services scarcity value and its response to urbanization in typical mountainous and hilly regions of south China. *Sci. Total Environ.* **2021**, *796*, 149032. [CrossRef]

15. Richardson, L.; Loomis, J.; Kroeger, T.; Casey, F. The role of benefit transfer in ecosystem service valuation. *Ecol. Econ.* **2015**, *115*, 51–58. [CrossRef]

16. Huang, L.; He, C.; Wang, B. Study on the spatial changes concerning ecosystem services value in Lhasa River Basin, China. Environ. *Sci. Pollut. Res.* **2022**, *29*, 7827–7843. [CrossRef]

17. Lu, H.T.; Huang, Q.Z.; Zhu, J.Y.; Zheng, T.C.; Yan, Y.; Wu, G. Ecosystem type and quality changes in Lhasa River Basin and their effects on ecosystem services. *Acta Ecol. Sin.* **2018**, *38*, 8911–8918. [CrossRef]

18. Xue, Y.X. Ecological Service Assessment of Lhasa River Basin Based on SWAT Model. Master's Thesis, North China Electric Power University, Beijing, China, 2020. [CrossRef]

19. Sun, N.; Chen, Q.; Liu, F.; Zhou, Q.; He, W.; Guo, Y. Land use simulation and landscape ecological risk assessment on the Qinghai-Tibet Plateau. *Land* **2023**, *12*, 923. [CrossRef]

20. Zhang, S.; Wu, T.; Guo, L.; Zhao, Y. Assessing ecological risk on the Qinghai-Tibet Plateau based on future land use scenarios and ecosystem service values. *Ecol. Indic.* **2023**, *154*, 110769. [CrossRef]

21. Wang, P.; Qin, S.T.; Hu, H.R. Spatial-temporal evolution characteristics of land use change and habitat quality in the Lhasa River Basin over the past three decades. *Arid Zone Res.* **2023**, *40*, 492–503. [CrossRef]

22. Yi, Y.; Zhang, C.; Zhu, J.; Zhang, Y.; Sun, H.; Kang, H. Spatio-temporal evolution, prediction and optimization of lUCC based on CA-Markov and InVEST models: A case study of Mentougou district, Beijing. *Environ. Sci. Pollut. Res.* **2022**, *19*, 2432. [CrossRef]

23. Mansour, S.; Al-Belushi, M.; Al-Awadhi, T. Monitoring land use and land cover changes in the mountainous cities of Oman using GIS and CA-Markov modelling techniques. *Land Use Pol.* **2020**, *91*, 104414. [CrossRef]

24. Xu, K.; Chi, Y.; Ge, R.; Wang, X.; Liu, S. Land use changes in Zhangjiakou from 2005 to 2025 and the importance of ecosystem services. *PeerJ* **2021**, *9*, e12122. [CrossRef]

25. Li, D.; Chang, Y.; Simayi, Z.; Yang, S. Multi-scenario dynamic simulation of urban agglomeration development on the Northern Slope of the Tianshan Mountains in Xinjiang, China, with the goal of high-quality urban construction. *Sustainability* **2022**, *14*, 6862. [CrossRef]

26. Zhu, K.; Cheng, Y.; Zang, W.; Zhou, Q.; El Archi, Y.; Mousazadeh, H.; Kabil, M.; Csoban, K.; David, L.D. Multiscenario simulation of land-use change in Hubei Province, China based on the Markov-FLUS model. *Land* **2023**, *12*, 744. [CrossRef]

27. Zhang, J.D.; Mei, Z.X.; Lv, J.H.; Chen, J.Z. Simulating multiple land use scenarios based on the FLUS model considering spatial autocorrelation. *J. Geo-Inf. Sci.* **2020**, *22*, 531–542.

28. Li, H.; Fang, C.; Xia, Y.; Liu, Z.; Wang, W. Multi-scenario simulation of production-living-ecological space in the Poyang Lake area based on remote sensing and RF-Markov-FLUS model. *Remote Sens.* **2022**, *14*, 2830. [CrossRef]

29. Liu, X.; Liang, X.; Li, X.; Xu, X.; Ou, J.; Chen, Y.; Li, S.; Wang, S.; Pei, F. A future land use simulation model (FLUS) for simulating multiple land use scenarios by coupling human and natural effects. *Landsc. Urban Plan.* **2017**, *168*, 94–116. [CrossRef]

30. Fu, B.J.; Zhang, L.W. Land-use change and ecosystem services:concepts, methods and progress. *Prog. Geogr.* **2014**, *33*, 441–446.

31. Ouyang, Z.Y.; Zheng, H. Ecological mechanisms of ecosystem services. *Acta Ecol. Sin.* **2009**, *29*, 6183–6188.

32. Ma, B.; Wang, X. What is the future of ecological space in Wuhan metropolitan area? A multi-scenario simulation based on Markov-FLUS. *Ecol. Indic.* **2022**, *141*, 109124. [CrossRef]

33. Zhang, X.; Ren, W.; Peng, H. Urban land use change simulation and spatial responses of ecosystem service value under multiple scenarios: A case study of Wuhan, China. *Ecol. Indic.* **2022**, *144*, 109526. [CrossRef]

34. Zhao, Q.; Shao, J. Evaluating the impact of simulated land use changes under multiple scenarios on ecosystem services in Ji'an, China. *Ecol. Indic.* **2023**, *156*, 111040. [CrossRef]

35. Wang, C.L.; Zhang, Y.L.; Wang, Z.F.; Bai, W.Q. Analysis of landscape characteristics of the wetland systems in the Lhasa River Basin. *Resour. Sci.* **2010**, *32*, 1634–1642. [CrossRef]

36. Brouwer, R. Environmental value transfer: State of the art and future prospects. *Ecol. Econ.* **2000**, *32*, 137–152. [CrossRef]

37. Repetto, R. Accounting for environmental assets. *Sci. Am.* **1992**, *266*, 94–101. [CrossRef] [PubMed]

38. Bai, W.Q.; Zhao, S.D. An analysis on driving force system of land use changes. *Resour. Sci.* **2001**, *23*, 39–41.

39. Li, P.; Li, X.B.; Liu, X.J. Macro-analysis on the driving forces of the land-use change in China. *Geogr. Resour.* **2001**, *20*, 129–138.

40. Cai, G.; Lin, Y.; Zhang, F.; Zhang, S.; Wen, L.; Li, B. Response of Ecosystem Service Value to Landscape Pattern Changes under Low-Carbon Scenario: A Case Study of Fujian Coastal Areas. *Land* **2022**, *11*, 2333. [CrossRef]

41. Xv, X.; Cheng, Y.; Jiang, H.; Li, X.; Liu, Y. Research progress of the effects of wind speed change on grassland ecosystem. *Acta Ecol. Sin.* **2017**, *37*, 4289–4298. [CrossRef]

42. Liu, Z.; Zhou, D.; Hao, L.; Fan, J.; Zhang, L. Uncertainty analysis of monitoring vegetation dynamics and driving factors in mountains based on multiple remote sensing indices: A case study of Nepal. *Environ. Ecol.* **2023**, *5*, 15–24.

43. Li, M.; Guan, J.; Zheng, J. Climate Drivers Contribute in Vegetation Greening Stalls of Arid Xinjiang, China: An Atmospheric Water Drying Effect. *Water* **2022**, *14*, 2019. [CrossRef]

44. Hagemann, S.; Blome, T.; Saeed, F.; Stacke, T. Perspectives in Modelling Climate–Hydrology Interactions. *Surv. Geophys.* **2014**, *35*, 739–764. [CrossRef]

45. Deepika, B.; Avinash, K.; Jayappa, K.S. Impact of estuarine processes and hydro-meteorological forcing on landform changes: A remote sensing, GIS and statistical approach. *Arab. J. Geosci.* **2015**, *8*, 711–726. [CrossRef]

46. Cai, D.; Ge, Q.; Wang, X.; Liu, B.; Goudie, A.S.; Hu, S. Contributions of ecological programs to vegetation restoration in arid and semiarid China. *Environ. Res. Lett.* **2020**, *15*, 114046. [CrossRef]

47. Chen, Z.; Huang, M.; Zhu, D.; Altan, O. Integrating remote sensing and a Markov-FLUS model to simulate future land use changes in Hokkaido, Japan. *Remote Sens.* **2021**, *13*, 2621. [CrossRef]

48. Roodposhti, M.S.; Hewitt, R.J.; Bryan, B.A. Towards automatic calibration of neighbourhood influence in cellular automata land-use models. *Comput. Environ. Urban Syst.* **2020**, *79*, 101416. [CrossRef]

49. Xu, Q.; Guo, P.; Jin, M.; Qi, J. Multi-scenario landscape ecological risk assessment based on Markov–FLUS composite model. *Geomat. Nat. Hazards Risk* **2021**, *12*, 1449–1466. [CrossRef]

50. Shi, J.; Shi, P.; Wang, Z.; Wang, L.; Li, Y. Multi-scenario simulation and driving force analysis of ecosystem service value in arid areas based on PLUS model: A aase study of Jiuquan city, China. *Land* **2023**, *12*, 937. [CrossRef]

51. Lou, Y.; Yang, D.; Zhang, P.; Zhang, Y.; Song, M.; Huang, Y.; Jing, W. Multi-scenario simulation of land use changes with ecosystem service value in the Yellow River Basin. *Land* **2022**, *11*, 992. [CrossRef]

52. Lu, T.; Li, C.; Zhou, W.; Liu, Y. Fuzzy assessment of ecological security on the Qinghai–Tibet Plateau based on Pressure–State–Response framework. *Remote Sens.* **2023**, *15*, 1293. [CrossRef]

53. Guo, N.; Degen, A.A.; Deng, B.; Shi, F.; Bai, Y.; Zhang, T.; Long, R.; Shang, Z. Changes in vegetation parameters and soil nutrients along degradation and recovery successions on alpine grasslands of the Tibetan plateau. *Agric. Ecosyst. Environ.* **2019**, *284*, 106593. [CrossRef]

54. Hafner, S.; Unteregelsbacher, S.; Seeber, E.; Lena, B.; Xu, X.; Li, X.; Guggenberger, G.; Miehe, G.; Kuzyakov, Y. Effect of grazing on carbon stocks and assimilate partitioning in a Tibetan montane pasture revealed by 13CO$_2$ pulse labeling. *Glob. Chang. Biol.* **2012**, *18*, 528–538. [CrossRef]

55. Li, Y.; Zou, J.; Zhang, L.; Sun, J. Aerobic granular sludge for simultaneous accumulation of mineral phosphorus and removal of nitrogen via nitrite in wastewater. *Bioresour. Technol.* **2014**, *154*, 178–184. [CrossRef] [PubMed]

56. Ma, R.F.; Liu, L.D.; Zhang, W.Z.; Li, J.M. Influencing factors and optimization path of sustainable development of plateau agriculture and animal husbandry—Taking Lhasa as an example. *J. Plateau Agric.* **2023**, *7*, 324–335. [CrossRef]

57. Wei, X.H.; Yang, P.; Dong, G.R. Agricultural development and farmland desertification in middle "One River and Its Two Branches" river basin of Tibet. *J. Desert Res.* **2004**, *24*, 196–200.

58. Yang, B.J.; Liu, H.T. Agricultural ecological environment and its protection in the central watershed of Tibetan "one River and two Rivers". *Res. Environ. Sci.* **1997**, *10*, 6. [CrossRef]

59. Pei, X. Flow Processes of Typical Ecosystem Services and Their Value Based on Data from Field Stations. Ph.D. Thesis, Institute of Geographic Sciences and Natural Resources Research, CAS, Beijing, China, 2013.

60. Li, S. Studies on the Flow Processes of Typical Ecosystem Services Based on Observation Network. Ph.D. Thesis, Institute of Geographic Sciences and Natural Resources Research, CAS, Beijing, China, 2010.

61. Gao, W.; Li, X.Y.; Zhang, Y.; Chen, Y. Evolution and prediction of ecosystem service values of the Yangtze River Basin. *Acta Ecol. Sin.* **2023**, *43*, 6203–6211.

62. Li, H.Y.; He, W.; Wang, J.Y.; Yang, S.Q.; Yao, Y.F. Multi-scenario prediction of ecosystem service value based on PLSR-FLUS-MarKov model—A case study of Lijiang River Basin. *J. Hydroecol.* **2023**, 1–14. [CrossRef]

63. Xie, G.D.; Lu, C.X.; Leng, Y.F.; Zheng, D.; Li, S.C. Ecological assets valuation of the Tibetan Plateau. *J. Nat. Resour.* **2003**, *18*, 189–196.

64. Xie, G.D.; Zhen, L.; Lu, C.; Xiao, Y.; Chen, C. Expert Knowledge Based Valuation Method of Ecosystem Services in China. *J. Nat. Resour.* **2008**, *23*, 911–919.

65. Zhang, T.H.; Wang, T.; Huang, Q.Z.; Wang, J.S.; Bao, X.T.; Liu, W.J.; Ding, L.B.; Li, C. Ecological risk assessment of Lhasa River Basin on the Tibetan Plateau. *Acta Ecol. Sin.* **2018**, *38*, 9012–9020. [CrossRef]

66. Yang, S.; Su, H.; Zhao, G.P. Multi-scenario simulation of urban ecosystem service value based on PLUS model: A case study of Hanzhong city. *J. Arid Land Resour. Environ.* **2022**, *36*, 86–95. [CrossRef]

67. Liu, W.H.; Zheng, J.W.; Wang, Z.R.; Li, R.; Wu, T.H. A bibliometric review of ecological research on the Qinghai–Tibet Plateau, 1990–2019. *Ecol. Inform.* **2021**, *64*, 101337. [CrossRef]

68. Liu, Z.C.; Feng, X.F.; Wu, S.; Kong, L.L.; Yao, X.C. Spatio-temporal dynamics of the urban-rural construction land and ecological land on Qinghai-Tibet Plateau. *J. Geo-Inf. Sci.* **2019**, *21*, 1207–1217.

69. Kang, S.; Xu, Y.; You, Q.; Fl U Gel, W.-A.; Pepin, N.; Yao, T. Review of climate and cryospheric change in the Tibetan Plateau. *Environ. Res. Lett.* **2010**, *5*, 015101. [CrossRef]

70. Wang, L.; Young, S.S.; Wang, W.; Ren, G.; Xiao, W.; Long, Y.; Li, J.; Zhu, J. Conservation priorities of forest ecosystems with evaluations of connectivity and future threats: Implications in the eastern Himalaya of China. *Biol. Conserv.* **2016**, *195*, 128–135. [CrossRef]

71. Wang, X.; Siegert, F.; Zhou, A.G.; Franke, J. Glacier and glacial lake changes and their relationship in the context of climate change, Central Tibetan Plateau 1972—2010. *Glob. Planet. Chang.* **2013**, *111*, 246–257. [CrossRef]

72. Yao, T.; Wang, Y.; Liu, S.; Pu, J.; Shen, Y.; Lu, A. Recent glacial retreat in High Asia in China and its impact on water resource in Northwest China. *Earth Sci.* **2004**, *47*, 1065–1075. [CrossRef]

73. Bolch, T.; Kulkarni, A.; Kääb, A.; Huggel, C.; Paul, F.; Cogley, J.G.; Frey, H.; Kargel, J.S.; Fujita, K.; Scheel, M.; et al. The state and fate of Himalayan glaciers. *Science* **2012**, *336*, 310–314. [CrossRef]

74. Immerzeel, W.W.; Van Beek, L.P.H.; Konz, M.; Shrestha, A.B.; Bierkens, M.F.P. Hydrological response to climate change in a glacierized catchment in the Himalayas. *Clim. Chang.* **2012**, *110*, 721–736. [CrossRef]

75. Sun, X.Y.; Zhang, R.J.; Huang, W.; Sun, A.; Lin, L.J.; Xu, H.G.; Jiang, D.C. The response between glacier evolution and eco-geological environment on the Qinghai-Tibet Plateau. *China Geol.* **2019**, *2*, 1–7. [CrossRef]

76. Xia, J.Y.; Lu, R.L.; Zhu, C.; Cui, E.Q.; Ying, D.; Huang, K.; Sun, B.Y. Response and adaptation of terrestrial ecosystem processes to climate warming. *Chin. J. Plant Ecol.* **2020**, *44*, 494–514. [CrossRef]